

Measuring Gravitational Redshifts in Galaxy Clusters

Nick Kaiser

Institute for Astronomy, University of Hawaii

2 November 2018

ABSTRACT

Wojtak *et al* have stacked 7,800 clusters from the SDSS survey in redshift space. They find a small net blue-shift for the cluster galaxies relative to the brightest cluster galaxies, which agrees quite well with the gravitational redshift predicted from GR. Zhao *et al.* have pointed out that, in addition to the gravitational redshift, one would expect to see transverse Doppler (TD) redshifts, so $\langle \delta z \rangle = -\langle \Phi \rangle + \langle \beta^2 \rangle / 2$ with β the 3D source velocity in units of c , and that these two effects are generally of the same order. Here we show that there are other corrections that are also of the same order of magnitude. The fact that we observe galaxies on our past light cone results in a bias such that more of the galaxies observed are moving away from us in the frame of the cluster than are moving towards us. This causes the observed average redshift to be $\langle \delta z \rangle = -\langle \Phi \rangle + \langle \beta^2 \rangle / 2 + \langle \beta_x^2 \rangle$, with β_x is the line of sight velocity. That is if we average over galaxies with equal weight. If the galaxies in each cluster are weighted by their fluence, or equivalently if we do not resolve the moving sources, and make an average of the mean redshift giving equal weight per photon, the observed redshift is $\langle \delta z \rangle = -\langle \Phi \rangle - \langle \beta^2 \rangle / 2$, so the kinematical effect is then opposite to the usual transverse Doppler effect. In the WHH experiment, the weighting is a step-function because of the flux-limit for inclusion in the spectroscopic sample and the result is different again, and depends on the details of the luminosity function and the SEDs of the galaxies. Including these effects substantially modifies the blue-shift profile. We identify some potential biases in the dynamical analysis of stacked clusters. We show that in-fall and out-flow have very small effect over the relevant range of impact parameters.

Key words: Cosmology: observations; galaxies: clusters: general

1 INTRODUCTION

Wojtak, Hansen and Hjorth (2011, hereafter WHH) have measured the gravitational redshift effect in clusters of galaxies. They stacked 7,800 massive clusters selected from the GMBCG cluster sample (Hao, J., *et al.*, 2010) derived from the SDSS DR7 survey data (Abazajian *et al.*, 2009) in redshift space, using coordinates of the brightest cluster galaxy (BCG) as the origin. They fit the cluster-frame redshift distributions, determined at a range of impact parameters, to a linear ramp to describe the foreground and background galaxies plus a quasi-Gaussian distribution to describe the cluster, and find that the centres of the cluster components have a small net blue-shift $\delta z \sim -10 \text{ km/s}/c$; a remarkable achievement since the galaxy clusters have velocity dispersions of order 600 km/s.

A blue-shift would be expected in GR since the light from the BCGs, which are thought to reside close to the centres of clusters, will have climbed out from deeper in the cluster potential well than the light from the majority of the galaxies, and the amplitude of the effect appears to be broadly consistent with their estimates of the gravitational

redshift obtained using a mean cluster mass distribution determined from the observed velocity dispersion.

WHH suggested that the result is in conflict with the predictions of TeVeS modified gravity theory (Bekenstein, 2004). However, agreement with the potential inferred from the kinematics of non-relativistic particles like galaxies is expected in any metric theory of gravity since both gravitational redshifts and particle motions are determined by the time component of the metric; what this type of measurement tests is the validity of the equivalence principle (Will, 2006; Bekenstein and Sanders, 2012; Zhao *et al.*, 2012, hereafter ZPL). This type of observation can, however, provide constraints on theories in which there are long-range non-gravitational interactions between dark matter that augments gravity on cluster scales (e.g. Gradwohl & Frieman, 1992; Gubser & Peebles, 2004; Farrar & Rosen, 2007).

WHH compare the frequency shift with the estimate for $\langle \Phi \rangle_{r_\perp} / c^2$ where the averaging is along a line of sight with impact parameter r_\perp . This would be appropriate if the light were emitted by non-inertial observers on a rigid, non-rotating, lattice in a state of rest with respect to the cluster. It is also valid, to a good approximation, for ob-

servations of the redshift of X-ray lines from heavy ions in the intra-cluster medium (Broadhurst & Scannapieco, 2000). But, as emphasised by ZPL, this is not correct when the light emanates from galaxies that are in free-fall. One way to obtain the observed redshift in this situation is to use local Lorentz boosts to give the Doppler shift between each emitting galaxy and its neighbouring lattice-based observer living in the rest-frame of the cluster (though there are other constructions one could use — see Bunn & Hogg (2009) for an in-depth discussion). If we set up coordinates such that the distant observer lives at positive x , the energy of a photon in the emitting galaxy’s frame relative to the cluster rest-frame is $E_G = \gamma(1 - \beta_x)E_{\text{RF}}$ where $\gamma = (1 - \beta^2)^{-1/2}$ and $\beta = \mathbf{v}/c$ with β_x the component towards the observer, so, up to second order in β the redshift is $1 + z = E_G/E_{\text{RF}} = 1 - \beta_x + \beta^2/2$. Adding the gravitational redshift difference yields the average redshift, given a phase-space density (PSD) for the galaxies $\rho(\mathbf{r}, \boldsymbol{\beta}, t)$, of

$$\langle \delta z \rangle = \frac{\int d^3r \int d^3\beta \rho(\mathbf{r}, \boldsymbol{\beta}, t) (-\beta_x + \beta^2/2 - \Phi/c^2)}{\int d^3r \int d^3\beta \rho(\mathbf{r}, \boldsymbol{\beta}, t)}. \quad (1)$$

Note that the redshifts here are all relative redshifts between observers and emitters in the vicinity of the cluster, not the redshift actually observed; i.e. $1 + z = (1 + Z_{\text{obs}})/(1 + Z_{\text{CL}})$.

If the cluster is virialised, the PSD will be an even function of velocity so the mean of the line-of-sight velocity β_x will vanish, and one would conclude that the mean redshift difference is

$$\langle \delta z \rangle = \langle z_G - z_{\text{BCG}} \rangle = \langle \beta_G^2 - \beta_{\text{BCG}}^2 \rangle / 2 - \langle \Phi_G - \Phi_{\text{BCG}} \rangle / c^2 \quad (2)$$

where now, following ZPL, allowance is made for the fact that the BCG will, in general, not be at rest at the centre of the cluster. Thus there is a positive contribution to the redshift, the transverse Doppler (TD) effect, that is opposite in sign to the gravitational redshift (GR) effect for rest-frame emitters (it being assumed here that the BCGs are on considerably lower energy orbits than the general cluster population) and, as emphasised by ZPL this effect will, quite generally, be of the same order as the gravitational redshift for a bound system by virtue of the virial theorem.

The point of this paper is to show that there are other corrections of the same order of magnitude. One arises from the fact that we observe the galaxies on our past light cone and this causes a bias such that we see more galaxies moving away from us than moving towards us. We show in §2 that this gives an additional redshift $\langle \beta_x^2 \rangle$.

But that is only true if each source galaxy is weighted equally in the averaging. If we apply any weighting based on galaxy luminosity then we also need to allow for the special relativistic beaming effect. In §3 we show that if we do not resolve the internal motions, but make an average that gives equal weight per observed photon, the resulting redshift is just the opposite of the transverse Doppler effect. That beaming and time-dilation would have an effect on gravitational redshift measurements using X-ray observations was noted by Broadhurst & Scannapieco (2000), but in that application it is a much smaller effect so was ignored.

In the WHH experiment the weighting was a step-function imposed by the flux-limit for inclusion in the spectroscopic sample. We calculate the effect of this in §4. This turns out to be the dominant kinematic effect.

In §5 we first attempt to clarify some issues concerning

dynamical analysis of a composite cluster formed by stacking a heterogeneous collection of clusters. We then apply these results together with the observed velocity dispersion profile to generate predictions for the net effect and compare with the observations.

In §6 we consider the effect of infall and outflow, which we find to have very little impact on the measurements, and in an appendix we develop the formalism for deriving, from numerical or analytical models, the predicted distribution of observed redshifts in order to facilitate a more direct comparison with the current and future observations.

2 PHASE-SPACE DENSITY ON THE PAST LIGHT-CONE

One might imagine that allowing for the light travel time would be simply a matter of replacing $\rho(\mathbf{r}, \boldsymbol{\beta}, t)$ in equation (1) by $\rho(\mathbf{r}, \boldsymbol{\beta}, t = x/c)$, in which case there would be no effect in the virialised region since for a stable, relaxed, system the PSD is independent of time. We are choosing the origin of time here to be the time the light we observe left the center of the cluster.

But this is not correct. While the PSD is invariant under Lorentz boosts and also along the trajectories of the particles, it has a non-trivial transformation from rest-frame to light-cone (LC) coordinates:

$$\rho_{\text{LC}}(\mathbf{r}, \boldsymbol{\beta}) = (1 - \beta_x) \rho_{\text{RF}}(\mathbf{r}, \boldsymbol{\beta}). \quad (3)$$

This means that the PSD for a virialised system viewed on the light cone is not an even function of velocity but has a small asymmetry which results in a non-vanishing of the mean of the line of sight component of the velocity.

One way to see how this arises is to consider taking a photograph of a swarm of particles where, in any region of space, there are as many particles moving towards us as away from us. The particles that we will see in a small cubical cell in space are not the same as the particles that occupy the cell at the moment the light passes through the centre of the cell. As the past light cone of the event of our opening the shutter sweeps towards us through the cell it will overtake more particles that are moving away from us than are moving towards us. The result is that more particles in the photograph will have positive radial velocities than negative ones. More quantitatively, if we have a pair of particles with the same x -component of velocity β_x with separation in the rest frame of dx then on our past light-cone they have a separation $dx_{\text{LC}} = dx_{\text{RF}}/(1 - \beta_x)$ and so the density (ordinary space density or phase-space density) on the light cone gains a factor $1 - \beta_x$. Note that this is a purely Newtonian plus light-travel-time effect, and has nothing to do with Lorentz-Fitzgerald length contraction which causes the density of particles to depend on the state of motion of the observer. It is the same effect that causes a runner on a trail to meet more hikers coming towards her than going in the same direction.

This result can easily be verified in the case of a toy model of a particle oscillating back and forth in a 1D parabolic potential well $\Phi(x) = \omega^2 x^2/2$. The trajectory is $x(t) = a \cos(\omega t + \phi)$, where ϕ is the phase. The velocity in the rest-frame of the potential trough is $\beta = -(a\omega/c) \sin(\omega t + \phi)$ which, on the light cone $t = x/c$ is $\beta =$

$-(a\omega/c)\sin(\omega x/c + \phi) \simeq -(a\omega/c)\sin\phi - (a\omega/c)^2\cos^2\phi$. The average of first term (over phase, or equivalently over time) vanishes, but the second term is always negative and is just $-\beta^2$, and the average agrees with $\langle\beta\rangle = \int dx \int d\beta \rho(x, \beta)(1-\beta)\beta / \int dx \int d\beta \rho(x, \beta)(1-\beta) = -\langle\beta^2\rangle$ with the rest frame PSD an even function of velocity.

For this toy model, and for particles uniformly distributed in phase, the PSD is zero except on a circle in (x', β) space (where $x' = x\omega/c$ is the dimensionless displacement), and $\rho(x', \beta, t)$ vanishes except on a cylinder around the t -axis. When we slice this cylinder on the light cone, the particles also live on a circle, but their density is non-uniform.

A parabolic 1-D potential is not very realistic, but the result is quite general. For particles orbiting in any static potential well, the average of the instantaneous line of sight velocity, either over time for one particle or over phase for a distribution, will average to zero, but the observed velocity will contain an extra term which is the light propagation time x/c times the acceleration of the particle, and the acceleration and position are anti-correlated in a gravitationally bound system, so this does not average to zero. Since the acceleration is the gradient of the potential, it is guaranteed that the average of the line-of-sight velocity will be of the same order as Φ/c .

WHH measured the mean redshift difference for galaxies at a range of projected distances r_\perp from the cluster center. The appropriate thing to compare with a PSD from a dynamical model or output of a numerical simulation is, with suitable normalisation,

$$\langle\delta z\rangle_{r_\perp} = \int dx \int d^3\beta \rho_{\text{RF}}(\mathbf{r}, \beta, t = x/c)(1 - \beta_x) \times (-\beta_x + \beta^2/2 - \Phi/c^2). \quad (4)$$

In the virialised region, this gives

$$\langle z - z_{\text{BCG}} \rangle = \langle \beta^2 - \beta_{\text{BCG}}^2 \rangle + \langle \beta^2 - \beta_{\text{BCG}}^2 \rangle / 2 - \langle \Phi_{\text{G}} - \Phi_{\text{BCG}} \rangle / c^2. \quad (5)$$

For isotropic orbits, the new term is 2/3 of the size of the TD effect and is of the same sign. Note that the asymmetry in the PSD applies to BCG as well; BCG line of sight velocities will also be biased to be positive with respect to the cluster centre of mass.

3 UNRESOLVED SOURCES

The foregoing analysis assumes that the redshift offsets are determined from a catalog of angular positions and redshifts, thus effectively giving equal weight per galaxy.

But when we cannot resolve the sources, such as when we try to allow for the kinematics of stars in BCGs, or, potentially, for low resolution H1 observations of clusters, we are averaging with equal weight per observed *photon*, and this changes the effect.

Consider a source that emits photons of fixed energy $E = E_0$ isotropically in its rest-frame in a burst as it passes the origin of space moving at velocity β along the x -axis. Boosting the photon 4-momenta into the 'laboratory frame' (denoted below by primed coordinates) one finds that a distant observer measures an energy $E(\mu') = E_0/\gamma(1 - \beta\mu') = E_0\gamma(1 + \beta\mu)$ where μ is the cosine of the

angle between the x -axis and the photon direction. Comparing the 3-momenta yields $\mu' = (\beta - \mu)/(1 + \beta\mu)$, and therefore the Jacobian of the transformation from observed to source-frame solid angles is $d\mu'/d\mu = 1/\gamma^2(1 + \beta\mu)^2 = (E_0/E)^2$, and since $n(\mu')d\mu' = n_0d\mu$, the density of photons per unit solid angle is $n(\mu') = n_0(E/E_0)^2 = n_0/\gamma^2(1 - \beta\mu')^2$. This is the familiar relativistic beaming effect. The energy is a function of lab-frame direction, and one finds that the probability distribution for energy is $P(E) \propto n(\mu')d\mu'/dE(\mu')$ which is flat from $E = E_0/\gamma(1 + \beta)$ to $E = E_0/\gamma(1 - \beta)$, and zero otherwise.

This is the probability distribution for random direction to the observer, or, equivalently, the probability distribution for a single observer viewing radiation from sources at the origin moving in random directions. It is also the same distribution one would find for a particle oscillating back and forth in a box, or for the emission from particles in a region of space if they are moving in randomly oriented directions though all at the same speed. The mean photon energy is readily found to be $\langle E \rangle = \int dE E P(E) = \gamma E_0$; a result that could have been anticipated since whatever rest-mass δm_0 the source used to create the radiation has energy in the lab-frame $\gamma\delta m_0 c^2$.

For a distribution of velocities we need to allow for the time-dilation effect: if the sources are identical and all emitting photons at a fixed rate in the frame, the interval between emission events in the observer-frame will be longer by a factor γ , so the number of photons observed per unit time from sources with gamma factor γ is $d\dot{n}(\lambda) \propto P(\gamma)d\gamma/\gamma$ and the average energy per photon is then

$$\langle E \rangle = \frac{\int d\dot{n} \gamma E_0}{\int d\dot{n}} = \frac{\int d\gamma \gamma E_0 P(\gamma)/\gamma}{\int d\gamma P(\gamma)/\gamma} = E_0 \langle \gamma^{-1} \rangle^{-1}. \quad (6)$$

We see here that the received energy per unit time is just the sum of the power of the sources, but the number of received photons per unit time in the observer frame has a $1/\gamma$ dependence.

For unresolved sources then, the effect of the internal kinematics is to introduce a blue-shift. How does this square with the result obtained in the previous section where we found that the effect for resolved sources was a red-shift that, once we allowed for light cone effects, was actually larger than the transverse Doppler effect? To see that the two calculations are consistent, and obtain a useful check of the validity of the light-cone effect, we now show that the resolved-source analysis reproduces the result for unresolved sources, as of course it should, if we introduce a weight per galaxy proportional to its fluence (number of photons per unit time per unit area at the detector). It is sufficient to consider identical isotropic emitters, for which the fluence is $dn/dt \sim En(E) \sim E^3$ where the extra factor of energy flux as compare to photon flux comes again from the transformation from intervals of time at the source and at the observer.

The number of photons per second received from such a source is proportional to $1/\gamma^3(1 - \beta\mu')^3$ and therefore the fluence weighted mean observed photon energy should be given by

$$\langle E \rangle = E_0 \frac{\int d\beta \beta^2 \rho_0(\beta) \int d\mu (1 - \beta\mu) \gamma^{-4} (1 - \beta\mu)^{-4}}{\int d\beta \beta^2 \rho_0(\beta) \int d\mu (1 - \beta\mu) \gamma^{-3} (1 - \beta\mu)^{-3}} \quad (7)$$

where the first factor of $1 - \beta\mu$ is the asymmetry of the ob-

served phase-space distribution from the light-cone effect, and where we have assumed that the distribution of velocities is isotropic and have dropped the prime. The integrals are elementary, and we readily find $\langle E \rangle = E_0/\langle 1/\gamma \rangle$, fully consistent with the result obtained above. Without the light-cone $1 - \beta\mu$ term we would have obtained a different result.

For non-relativistic systems with $\beta^2 \ll 1$ the effect of the internal motions of emitters within unresolved objects is to give a change of energy $\delta E/E_0 \simeq \langle \beta^2 \rangle/2$ which is a blue-shift and just opposite to the usual transverse Doppler redshift.

4 SURFACE BRIGHTNESS MODULATION

In §2 we implicitly assumed that all galaxies are observed and catalogued. But in reality the galaxies in the spectroscopic sample were selected according to their apparent luminosities. As discussed in §3, a galaxy's apparent luminosity depends on its state of motion through the beaming effect which changes the surface brightness and hence luminosity. This results in a bias for the redshifts of the cluster galaxies which are selected for redshift measurement as the surface brightness modulation means that galaxies moving away from us in a given region of space have a higher limit on their intrinsic luminosities than galaxies moving towards us. For the WHH experiment the effect is quite strong, and strongly increasing with cluster redshift, since the flux limit ($r = 17.8$) is only about one magnitude fainter than M_* even at the minimum redshift limit, so the flux selection limit falls on the steep end of the luminosity function (LF) where small fractional changes in luminosity have a large effect on the number of sources detected.

We then consider the effect on the BCGs. For these the flux limit is irrelevant, but there is a bias because velocities can change the ranking of the two brightest galaxies. This turns out to be almost independent of cluster redshift.

4.1 Flux-Limited Galaxies

For low velocities $\beta \ll 1$ the fractional change of the fluence is $\Delta\dot{n}/\dot{n} = 3\beta_x$, but to obtain the observed photon count, we also need to allow for the change in frequency and the limits imposed by the broad-band filter. Combining these, the fractional change in apparent luminosity for a galaxy in a cluster at redshift Z is $\Delta l/l = (3 + \alpha(Z))\beta_x$, where the effective spectral index, for a photon counting detector with response curve $R(\lambda)$, is $\alpha(Z) = -d\ln(\int d\lambda \lambda R(\lambda)/(1+Z))f_\lambda/d\ln(1+Z)$. This depends on the details of the galaxy SED, but is found, using SEDs for E, S0 and Sb galaxies from Coleman, Wu and Weedman (1980) to be close to 2 for galaxies at the relevant redshifts (see figure 1), reflecting the fact that in the r -band, galaxies tend to have flat f_λ curves.

The modulation of the number density of detectable objects is given by the product of $\Delta l/l$ and the logarithmic derivative $\delta(Z) \equiv -d\ln n(> L_{\text{lim}}(Z))/d\ln L$ which, as mentioned, is a strongly increasing function of redshift. Ideally we would calculate this using a luminosity function appropriate for the actual cluster galaxies used in the study, and this will, in general, depend on the projected distance from the cluster center. However, Hansen *et al.* (2009) have shown that while the mix of red *vs.* blue galaxies changes

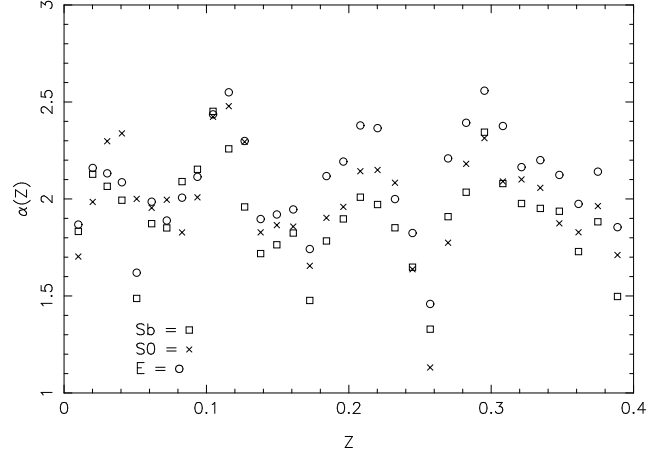


Figure 1. Spectral index vs. redshift for representative galaxy types observed in Sloan r -band

strongly with radius, the overall luminosity function does not vary much, and the parameters are not very different from the field galaxy luminosity function, so we will use the latter, as determined for SDSS by Montero-Dorta & Prada (2009), as a proxy. Their estimate of the LF obtained from the r -band magnitudes K -corrected to $Z = 0.1$ has $M_* - 5\log_{10} h = -20.7$ and faint end slope of $\alpha = -1.26$. The resulting $d\ln n(> L)/d\ln L$, computed using the flux limit $r = 17.77$ appropriate for the SDSS spectroscopic sample used by WHH, is shown as the dot-dash curve in figure 2.

Finally, we need the average of $-(3 + \alpha)d\ln n(> L)/d\ln L$ over the redshift distribution for the galaxies actually used in the experiment. The 7,800 clusters used by WHH were selected by applying a richness limit to the parent GMBCG catalog (Hao, J., *et al.* 2010) that contains 55,000 clusters extending to $Z = 0.55$. These clusters were derived from the SDSS photometric catalog that is much deeper than the spectroscopic catalog. Consequently, at the redshifts where the spectroscopically selected galaxies live, this parent catalog is essentially volume limited for the clusters used, so the redshift distribution for the cluster members used is essentially the same as that for the redshift distribution for the entire spectroscopic sample, save for the fact that the GMBCG catalog has a lower redshift limit $Z_{\text{lim}} = 0.1$, which is very close to the redshift where $dN/dZ = Z^2 n(Z)$ peaks. This is the bell shaped curve in figure 2. Combining these we find $\langle d\ln n/d\ln L \rangle = \int dZ Z^2 n(Z) d\ln n/d\ln L / \int dZ Z^2 n(Z) \simeq -2.0$ with integration range $0.1 < Z < 0.4$, and the average $-\langle (3 + \alpha(Z))d\ln n(> L)/d\ln L \rangle \simeq 10$. This may be a slight overestimate, as the cluster catalogue is not precisely volume limited and the actual dN/dZ may lie a little below the solid curve in figure 2 at the highest redshifts.

For the WHH experiment, the surface brightness modulation effect is considerably larger in amplitude than the transverse Doppler and light-cone effects, but has opposite sign. For isotropic orbits the combination of the TD, LC and SB effects is

$$\langle \delta z \rangle = (2.5 - \langle (3 + \alpha(Z))\delta(Z) \rangle) \langle \beta_x^2 \rangle \simeq -7.5 \langle \beta_x^2 \rangle. \quad (8)$$

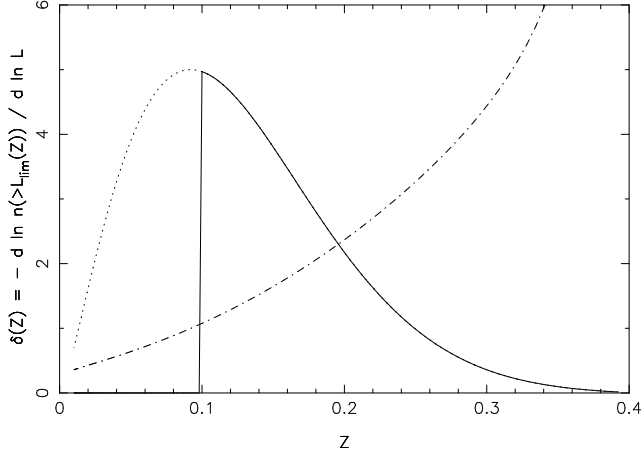


Figure 2. The dot-dash curve is the logarithmic derivative of the comoving density of objects above the luminosity limit as a function of redshift. The bell-shaped curve is $dN/dZ = Z^2 n(Z)$ and the solid curve is that truncated at the minimum redshift imposed by the parent cluster catalogue. The mean of the log-derivative, averaged over the redshift distribution turns out to be ≈ 2.0 .

4.2 Effect on BCGs

The TD and LC effects act on all galaxies, including the BCGs, in the same way. The SB effect is different; in the WHH analysis, only clusters with at least 5 measured redshifts were used, so it is safe to assume that the brightest cluster galaxies will be unaffected by the flux limit. However, for some small fraction of the clusters, the two brightest galaxies will have magnitudes that are sufficiently close that the effect of surface brightness modulation by the motions will be enough to change their ranking, resulting in a bias. In principle, this effect could be eliminated by only using clusters where the difference between the two brightest galaxies is sufficiently large that the velocities cannot change the ranking.

To analyse this, let the joint distribution of difference of intrinsic magnitudes $m_{ab} = m_a - m_b$, and line-of-sight velocities β_a, β_b for pairs of top two ranked cluster galaxies, in no particular order, be $P_0(m_{ab}, \beta_a, \beta_b)$. This is a symmetric function of m_{ab} .

The velocities change the observed surface brightnesses of the galaxies, and hence the difference of observed magnitudes is $m'_{ab} = m_{ab} - \kappa(\beta_a - \beta_b)$, where $\kappa \equiv (\ln(10)/2.5)(3 + \alpha(Z))$, so the observed distribution is $P(m_{ab}, \beta_a, \beta_b) = P_0(m_{ab} - \kappa(\beta_a - \beta_b), \beta_a, \beta_b)$, the Jacobian of the transformation from intrinsic to observed magnitude being unity.

The probability distribution for the velocity of the first ranked galaxy β_1 is then

$$P(\beta_1) = \int_{-\infty}^0 dm_{ab} \int_{-\infty}^{\infty} d\beta_b P(m_{ab}, \beta_1, \beta_b) + \int_0^{\infty} dm_{ab} \int_{-\infty}^{\infty} d\beta_a P(m_{ab}, \beta_a, \beta_1) \quad (9)$$

i.e. the sum of the distribution function for β_a if $m_{ab} < 0$ and the DF for β_b if $m_{ab} > 0$.

Making a Taylor expansion of $P(m_{ab}, \beta_a, \beta_b)$ with re-

spect to m_{ab} and performing the integrals yields

$$P(\beta_1) = P_0(\beta_1) - 2\kappa\beta_1 P_0(m_{ab} = 0, \beta_1) \quad (10)$$

which depends on the joint distribution of the intrinsic magnitude difference and the velocity of one or other of the two brightest galaxies. The mean redshift offset is then

$$\langle \delta z_{\text{BCG}} \rangle = -\kappa \sigma_{ab}^2 P_0(m_{ab} = 0) / c^2 \quad (11)$$

where $\sigma_{ab}^2 \equiv \langle (\beta_a - \beta_b)^2 | m_{ab} = 0 \rangle$ is the variance of the relative velocity of the two brightest galaxies given that they have similar magnitudes. This is something that is straightforward to measure from the data. It is reasonable to expect that this is larger than (twice) the velocity variance for brightest cluster galaxies. Smith *et al.* (2010) have measured the distribution for magnitude differences and find $P_0(m_{ab} = 0) \approx 0.35$ so we then have

$$\begin{aligned} \langle \delta z_{\text{BCG}} \rangle &\approx 0.32(3 + \alpha(Z)) \sigma_{ab}^2 / c^2 \\ &\approx 1.9 \text{ km/s/c} (\sigma_{ab} / 600 \text{ km/s})^2. \end{aligned} \quad (12)$$

Note that the surface brightness boosting effect on BCGs does not have the strong redshift dependence that is expected for the flux-selected galaxies.

5 PREDICTING THE REDSHIFT PROFILE

We can now make a prediction for the combined GR+TD+LC+SB effect as a function of radius using the observed velocity dispersion data provided by WHH. We start with a discussion of dynamical analysis of a composite, or stacked, cluster and how this differs from the analysis of single cluster. We then review the relevant properties of the BCGs; both their cluster-centric kinematics and their halo properties. We then attempt to combine all of the effects discussed above to predict the expected profile of the redshift offset.

5.1 The Gravitational Redshift

A composite cluster differs from a single cluster in several ways. Individual clusters are very much still in the process of forming and so tend to be unrelaxed and to have strong substructure. They can also undergo very strong fluctuations in density and potential as they go through the process of merging. In the composite, any such fluctuations and substructure will be averaged out, and the form of the composite can, in the limit of large number of contribution clusters, be assumed to be nearly spherically symmetric — more precisely the composite will have symmetry about the line-of-sight axis but may have some elongation along the line of sight — and can evolve only on a cosmological timescale. These are obviously beneficial differences; the usual assumptions of stability and symmetry which apply only poorly to individual clusters should be well obeyed for a composite.

In an individual single cluster, the gravitational potential is a function of position and time. In the composite constructed by WHH, the individual clusters span more than an order of magnitude in range of mass, so galaxies at the same position in the composite will be subject to very different gravitational accelerations, and there will also be fluctuating forces that can, for example, stochastically heat a particle

from a low energy orbit to a higher energy one, as happens as a result of violent relaxation during merging (Lynden-Bell, 1967). Consequently, unlike an individual cluster where the galaxies behave like a fluid in phase-space, the galaxies in the composite behave like a gas where initially neighbouring particles will later be found to be widely separated. The galaxies in a composite therefore do not obey the Vlasov (or collisionless Boltzmann) equation, which is usually the starting point for derivation of the equations of continuity for matter and momentum that allow one to relate density, potential and velocity dispersions.

Nonetheless, a composite has a velocity dispersion tensor and a gravitational potential, both functions of position, and both of whose projections are observable. Each is some kind of average over the cluster population. But, given the large range in cluster masses, and the issue of how the centres of the clusters were determined in order to do the stacking, the question of how exactly these are related is non-trivial.

WHW modeled both of these observables as being the averages one would obtain for spherical clusters with a power law distribution in virial mass, truncated at the same limits as used in selecting the clusters, and having NFW model (Navarro *et al.*, 1997) profiles. The amplitude and index of the mass function and the NFW concentration parameter were treated as free parameters determined by matching the predicted velocity dispersion to that observed. The mass-anisotropy degeneracy issue was addressed by performing the modeling for two values of the anisotropy parameter $\beta = 1 - \sigma_\theta^2(r)/\sigma_r^2(r) = 0, 0.4$ which span the range suggested by simulations and observations. The effect of using BCGs as centres was incorporated in the model by boosting the line-of-sight model velocity dispersions by adding the BCG velocity dispersion in quadrature: $\sigma^2(r_\perp) \rightarrow \sigma^2(r_\perp) + \sigma_{\text{BCG}}^2$ with σ_{BCG} assumed to be 35% of the total velocity dispersion.

Here we show that there is a more direct way to relate the velocity dispersion and the potential that does not require any modelling of the mass function of the clusters. We find that the velocity moments determined from the composite obey Euler's equation and directly provide, without any correction for motions of the BCGs, the average gravity, relative to the BCG, as a function of distance from the BCG. This is almost exactly what is needed to predict the gravitational redshift of galaxies relative to the BCG, which is what is measured. Advantages of this approach are simplicity, and that it allows a non-parametric reconstruction of the gravity which, given the great precision of the velocity dispersion data, is eminently practical and obviates the need for assumptions about the profiles of the clusters. If clusters were individually spherical this analysis would be exact. The only problem is that Euler's equation provides the average *gravity* weighted by galaxy number, whereas the gravitational redshift is the average *potential* weighted by galaxy number. The gradient of the latter is not precisely equal to the former; so the relationship suffers an asphericity bias. This bias can be estimated from simulations or, in principle, from the projected shapes of the actual clusters used in the measurement. Here we use a simple analytic model with realistic quadrupole moments for the density to show that the effect of this kind of low-order cluster asphericity is in fact very small. Displacement of the BCG from the centre

of mass of the cluster also introduces asphericity. This produces a bias that falls off rapidly with distance, but may be important at small impact parameter.

Let us assume as our fundamental model for galaxies that for a cluster, with mass, size, shape, orientation etc. denoted by label C , there is a phase-space distribution function $\rho_{CG}(\mathbf{r}, \mathbf{v})$ that is in general dependent on the type and luminosity of the galaxy denoted by an abstract index G ; that the observed galaxies are a Poisson sample of this density field, and that $\rho_{CG}(\mathbf{r}, \mathbf{v})$ obeys the collisionless Boltzmann equation. The idea here is that things like dynamical friction and response to the cluster environment happen slowly, at least in an ensemble average sense, and that the instantaneous relation between the phase-space coordinates is the same as for massless test particles. The PSDF is interpreted here as a probability density (e.g. Binney & Tremaine, 2008).

Consider a composite cluster constructed by making a big realisation of clusters drawn from a probability distribution function $P(C)$ for the cluster attributes and with galaxies generated from the distribution function to make a big synthetic redshift survey; selecting clusters by some suitably defined cluster identification algorithm and then stacking them in redshift space relative to suitably defined centres. These might be defined, as in WHH, as the locations of the most luminous galaxies that are likely to lie near the bottom of the cluster potential well. Alternatives would be to define the origin as some kind of centroid of the redshift-space coordinates of the galaxies in each cluster, or one might use the X-ray centroid to give the angular position on the sky.

At any position \mathbf{r} relative to the centre of some cluster C , the zeroth, first and second moments of the velocity over the PSDF obey the time dependent Euler equation:

$$\partial_t(n\langle v_i \rangle) + \partial_j(n\langle v_i v_j \rangle) + n\partial_i\Phi = 0 \quad (13)$$

where, as usual, $n = \int d^3v \rho(\mathbf{r}, \mathbf{v})$, $\langle v_i \rangle = n^{-1} \int d^3v \rho(\mathbf{r}, \mathbf{v}) v_i$ etc., and all are understood to be dependent on the particular choice of cluster and tracer type G and Φ is determined by the cluster only. This is valid in coordinates that are relative to the instantaneous position and velocity of the centre, and Φ_C may also be defined to be relative to the potential at the spatial origin.

The Euler equation is an expression of the conservation of momentum. This may also be obtained directly from the stress, or momentum flux, tensor. For a Newtonian gravitating system composed of a large-number of particles the stress has both a kinetic component and a contribution from the gravitational field:

$$T_{ij} = \sum_G m_G n_{CG} \langle v_i v_j \rangle_{CG} + \frac{1}{4\pi G} (g_i g_j - \delta_{ij} g^2/2) \quad (14)$$

(Maxwell, 1875; Misner, Thorne & Wheeler, 1973), G here being generalised to include the dark matter particles and $g_i = -\partial_i \Phi_C$. The momentum density is $T_i^0 = \sum_G m_G n_{CG} \langle v_i \rangle_{CG}$ and conservation of momentum: $T_{i,\mu}^\mu = 0$ is

$$\sum_G m_G [\partial_t(n_{CG} \langle v_i \rangle_{CG}) + \partial_j(n_{CG} \langle v_i v_j \rangle_{CG}) + n_{CG} \partial_i \Phi_C] = 0. \quad (15)$$

In general, the quantity in parentheses [...] need not vanish for every component, only the mass-weighted sum has to

vanish. For example, in a thermal, ionised plasma, the kinetic stress for both components is the same, the velocity dispersions scaling inversely with mass, while the gravity acts primarily on the ions. Here the electromagnetic interaction allows the transfer of momentum between the two components. For collisionless particles, which we are assuming galaxies mimic, there is no way for different species to exchange momentum and the Euler equation is obeyed separately for each of the independent components.

The zeroth, first and second velocity moments for the composite at position \mathbf{r} are

$$\begin{aligned} n_G &= \int dCP(C)n_{CG} \\ n_G \langle v_i \rangle_G &= \int dCP(C)n_{CG} \langle v_i \rangle_{CG} \\ n_G \langle v_i v_j \rangle_G &= \int dCP(C)n_{CG} \langle v_i v_j \rangle_{CG} \end{aligned} \quad (16)$$

where $P(C)$ is the probability density for clusters as a function of size, shape, orientation etc. We then have

$$\partial_t(n_G \langle v_i \rangle_G) + \partial_j(n_G \langle v_i v_j \rangle_G) = \int dCP(C)[\partial_t(n_{CG} \langle v_i \rangle_{CG}) + \partial_j(n_{CG} \langle v_i v_j \rangle_{CG})] \quad (17)$$

but [...] is, by equation (13) just $-n_{CG} \partial_i \Phi_C$ so

$$\partial_t(n_G \langle v_i \rangle_G) + \partial_j(n_G \langle v_i v_j \rangle_G) = n_G \bar{g}_{Gi} \quad (18)$$

where

$$\bar{g}_{Gi} \equiv -\frac{\int dCP(C)n_{CG} \partial_i \Phi_C}{\int dCP(C)n_{CG}} \quad (19)$$

which is the galaxy number weighted mean gravity relative to the BCGs.

The moments determined from the composite therefore satisfy Euler's equations for particles moving in a potential whose gradient is (minus) the galaxy weighted mean gravity. In equilibrium, the rate of change of the momentum density must vanish, the pressure and gravitational stress tensors adjusting themselves so that the divergence of the total momentum flow vanishes. That the kinetic pressure gradient should accurately balance the gravitational force density is essentially guaranteed regardless of how the centres are chosen. For example, one might select gas rich galaxies as centres, and these will have a tendency to be falling into the cluster for the first time. There will therefore be a net momentum density for the general cluster galaxies relative to these centres: $n \langle v_i \rangle \neq 0$. But as all ensemble average properties of the cluster population can evolve only on a cosmological time-scale, the rate of change of the momentum density is $\partial_t(n \langle v_i \rangle) \sim H n \langle v_i \rangle$ which is smaller than either the kinetic or gravitational stress divergence by the ratio of the dynamical time to the Hubble time. Thus, even for this rather extreme choice of 'centres', at the virial radius one would expect at most a small $\sim 10\%$ force imbalance.

If we ignore the line-of-sight elongation from cluster selection effects, the composite density, potential etc. will all be spherically symmetric and the mean gravity will be radially directed. For a spherical system, the kinetic stress tensor for the G th component (divided by m_G) is $T_{ij}^{(k)} = n((\sigma_r^2 - \sigma_\perp^2)\hat{x}_i \hat{x}_j + \sigma_\perp^2 \delta_{ij})$, where σ_r and σ_\perp are the radial and tangential velocity dispersions, and its divergence

is $\partial_i T_{ij}^{(k)} = \hat{x}_j(\partial_r(n\sigma_r^2) + 2n(\sigma_r^2 - \sigma_\perp^2)/r)$ so

$$\partial_r(n\sigma_r^2) + 2n(\sigma_r^2 - \sigma_\perp^2)/r - n\bar{g} = 0 \quad (20)$$

the familiar form for Euler's equation for a spherical equilibrated system.

If we assume some velocity dispersion anisotropy, we can, in principle, de-project the projected density and velocity dispersion to obtain $n(r)$ and σ_r from which the Euler equation provides the radially directed gravity vector $\bar{g}(r)$.

The gravitational redshift is the projection of the galaxy weighted average 3-D potential, relative to the cluster centre,

$$\bar{\Phi} = \frac{\int dCP(C)n_{CG}\Phi_C}{\int dCP(C)n_{CG}} \quad (21)$$

which is obviously very closely related to the gravity vector furnished by the Euler equation (19).

This is all very nice, but the catch is that for real clusters with asymmetry and substructure the potential that one obtains by integrating the galaxy number weighted average gravity will not be precisely equal to the galaxy weighted average potential. Therefore predicting the gravitational redshift from the observed velocity dispersion is more complicated than for an individual relaxed spherical cluster. The problem here is that the observable properties, being averages of the gravity or potential weighted by galaxy number, are biased by asphericity of the clusters. Part of this asphericity comes from the fact that BCGs do not in general lie at the minimum of the potential, but the biases will be present even in the limit of very cold reference galaxies.

The above analysis has focused on recovering the potential from the velocity dispersions alone. This was the approach taken by WHH, in fitting the velocity dispersion profile to a parameterised model of stacked NFW models. Kinematic data have the advantage, modulo velocity anisotropy issues, of providing an unbiased view of the mass, but relying on the kinematic data alone, and imposing constraints on the form of the model, is potentially dangerous. If BCGs do not lie at the centres of clusters, and indeed there is considerable evidence that they have substantial displacements, then a NFW model with its $\rho \sim 1/r$ central cusp would not be a good model for the number density profile around the BCGs, which will have a core.

The NFW model predicts that the velocity dispersion falls at very small impact parameter where we see low-energy galaxies trapped deep in the central conical potential well. Unfortunately the data presented in WHH supplementary figure 2 do not have sufficient resolution to reveal whether this is or is not obeyed. The data show the velocity dispersion to be very flat for $r_\perp \lesssim 0.5\text{Mpc}$ and do not allow one to discriminate between a core caused by finite energies of BCGs and a cusp. If there is a core, then the predicted GR effect will be reduced. We will attempt to estimate this below. The NFW model is also not appropriate at large radius. The density in the model falls off as $\sim 1/r^3$ whereas we know from measurements of the cluster-galaxy cross-correlation function that, to the extent that galaxies are fair tracers of the mass, the real profile is more like $1/r^2$. A more reliable approach would be to use the kinematics and the projected density profile to determine a mass-per-galaxy M at around the virial radius, preferably correcting for the asphericity biases, and then use the inverse Laplacian of the galaxy num-

ber density to predict the gravitational potential. This could be done using parameterised models, but if so, these should be allowed to have realistic profiles.

Poisson's equation being linear, the Laplacian of the ensemble (spatial) average of the potential at position \mathbf{r} relative to the centre is

$$\nabla^2 \Phi(\mathbf{r}) = 4\pi G M_G \frac{\int dCP(C) n_{CG}(\mathbf{r})}{\int dCP(C)} = 4\pi G M_G n_G(\mathbf{r}) \quad (22)$$

which is spherically symmetric. Inverting this gives the spatial average potential, relative to the centre, $\Phi(\mathbf{r}) = 4\pi G M_G \nabla^{-2} n_G(\mathbf{r})$. But using this to predict the gravitational redshift also gives an asphericity biased result since the quantity one measures is

$$\bar{\Phi} = 4\pi G M_G \frac{\int dCP(C) n_{CG} \nabla^{-2} n_{CG}(\mathbf{r})}{\int dCP(C) n_{CG}} \quad (23)$$

and again the inverse Laplacian operator does not commute with the averaging if the clusters are non-spherical.

These biases are something of a nuisance. However, there is some reason to think that they are quite small for realistic clusters. Kasun and Evrard (2005) have studied the shapes of clusters in numerical simulations. They compute second moments of the distribution of particles within r_{200} and find that for massive clusters (virial mass greater than $3 \times 10^{14} M_\odot$) the modal minor/major axis ratio — the square root of the ratio of the smallest to largest eigenvalues of the 2nd moment matrix — is about 0.64, and they find that smaller clusters are rounder.

A simple model that would reproduce this is a softened tri-axial isothermal sphere potential $\Phi = \ln(C_{ij} x_i x_j + r_c^2)$. At three times the core radius this has density with second moments that reproduce the numerical results if we take $C_{ij} = \text{diag}\{1.2, 1, 1/1.2\}$. However, the biases are then very small; less than one percent for the radial component of the gravity and about 3 percent for the potential. This analysis only considers the lowest order quadrupole shape anisotropy, and does not address the effect of the displacement of the BCG from the potential minimum. The latter, however, produces a dipole anisotropy for the density, radial gravity, potential etc., but these decrease with increasing radius, so the bias is a strongly decreasing function of radius. While the rms displacements of the BCGs are, of course, related to their cluster-centric velocity dispersion, the bias, cannot be compensated for by simply adding the BCG velocities in quadrature to the model velocities as that has effectively the same effect at all radii.

Clearly what is needed is an estimate of the biases from numerical simulations, though it is also possible to attack this observationally using the shapes of real clusters seen in projection. If the results of this simple analytical model are supported, then the conclusion is that the composite cluster can be analysed almost exactly as though one were dealing with a single spherical equilibrated cluster, and that one can reconstruct the potential in the virialised region from Euler's equation — using velocity dispersions exactly as observed, and without any correction for the BCG velocity dispersion — and then armed with the mass-per-galaxy factor the potential can be determined at larger and smaller scales using the de-projected galaxy distribution.

5.2 BCG Properties

5.2.1 Intra-cluster Kinematics

The analysis of WHH relies on the assumption that, in an average sense, the BCGs used as the origin of coordinates in velocity and angle space are a relatively cold population, velocity-wise, compared to the other galaxies and are therefore orbiting close to the potential minimum. There are good theoretical grounds for believing that the BCGs will indeed be colder than the general population, but understanding in detail just how cold they are is important here for two reasons: first because the kinematically sourced effects depend on the velocity dispersions of the BCGs and second because it can inform us to what extent the mean density profile around the BCG is in fact likely to depart from the idealised NFW model predictions.

WHH assume $\sigma_{\text{BCG}} = 0.35\sigma_{\text{obs}}$, citing Skibba *et al.* (2011), in which case the effect on estimates of e.g. the TD and LC effects is quite small. But this may be a bit low. Skibba *et al.* found that the velocity dispersion for the *central* galaxies in the clusters were $\sigma_{\text{cen}} \simeq 0.5\sigma_{\text{CL}}$ which is a lot larger, but not directly measuring the same thing since they also found that about 30% of the time, the central galaxy was not in fact the brightest galaxy in the cluster.

Coziol *et al.* (2009) have measured the distribution of BCG motions directly and find that $\langle |v_{\text{BCG}}| \rangle / \sigma_{\text{CL}} \simeq 0.40 \pm 0.04$ for clusters of Abell richness class $R=1$. These clusters have mean dispersion $\sigma = 651 \text{ km/s}$, a little higher than for the composite cluster here. The mean dispersion for $R=0$ is $\sigma = 539 \text{ km/s}$, for which they find $\langle |v_{\text{BCG}}| \rangle / \sigma_{\text{CL}} \simeq 0.43 \pm 0.03$ so the appropriate value for the sample here is around 0.42.

For a Gaussian distribution, $\langle |v_{\text{BCG}}| \rangle = \sqrt{2/\pi} \sigma_{\text{BCG}}$ so this suggests $\sigma_{\text{BCG}} = 0.53\sigma_{\text{CL}}$ which is again considerably larger than the value adopted by WHH and consistent with what Skibba *et al.* found for the central cluster galaxies.

If we define $\alpha \equiv \sigma_{\text{BCG}}^2 / \sigma_{\text{CL}}^2$ then we have $\sigma_{\text{CL}}^2 = \sigma_{\text{obs}}^2 / (1 + \alpha)$ and $\sigma_{\text{BCG}}^2 = (\alpha / (1 + \alpha)) \sigma_{\text{obs}}^2$. For $\alpha = 0.25$, as suggested by the observations, and $\sigma_{\text{obs}} = 610 \text{ km/s}$ we have $\sigma_{\text{BCG}} = 270 \text{ km/s}$ and $\sigma_{\text{CL}} = 545 \text{ km/s}$. With this value the differential TD and LC effects are reduced to about 60% of what one would expect in the limit that the BCGs lie at rest at the minimum of the cluster potential. The SB effect, as we show below, is somewhat less affected.

We can also estimate the reduction in the gravitational redshift, assuming that the clusters in which the BCGs live do indeed have NFW profiles. Vanishing of the second time derivative of the moment of inertia $I = \sum r^2$ tells us that $\langle |\dot{r}|^2 \rangle = 3\sigma_{\text{BCG}}^2 = \langle r |\nabla \Phi| \rangle$. In the inner parts of the NFW profile, the potential increases linearly with radius, so consequently we have $\langle r |\nabla \Phi| \rangle = \langle \Phi \rangle$ so the predicted gravitational blue-shift for the hot population relative to the colder BCG population is decreased by $\delta z = 3\sigma_{\text{BCG}}^2 / c^2 \simeq 0.9(\sigma_{\text{BCG}}/300 \text{ km/s})^2 \text{ km/s/c}$. But their motions will also give them TD and LC red-shifts that are $\delta z \simeq 2.5\sigma_{\text{BCG}}^2 / c^2$ which largely counteracts the change in the GR effect, and from §4.2 the SB effect on the BCGs gives them a blue shift which we have estimated to be about $c\delta z = -1.9 \text{ km/s}$.

Finally, one should allow for the fact that the light we see from the galaxies will have suffered gravitational redshift escaping the halos of the galaxies, and that the starlight will

also be affected by stellar motions as described above in §3. This is most important for the BCGs.

5.2.2 BCG Halo and Internal Kinematics

Regarding the GR effect, the stellar velocity dispersion in BCGs is typically $\sigma_* \sim 250$ km/s (e.g. Bernardi *et al.*, 2007); much larger than that of the run-of-the-mill galaxies, and quite comparable to the motion of the BCGs in the cluster halo. The BCGs are unresolved, so we can use the result of §3 to predict the kinematically sourced blue-shift $\delta z \sim -(3/2)(\sigma_*/c)^2 \sim -0.3$ km/s/c, which is quite small. If they have flat rotation curve halos, for which $\Phi = \Phi_0 \ln r$ then, for isotropic orbits, $\Phi_0 = 2\sigma_{DM}^2$ while vanishing of \ddot{I} for the stars requires $\Phi_0 = 3\sigma_*^2$. The gravitational redshift is therefore $\delta z = 3(\sigma_*^2/c^2)\langle \ln(r_{\text{halo}}/r_*) \rangle = 0.63 \text{ km/s/c} (\sigma_*/250 \text{ km/s})^2 \langle \ln(r_{\text{halo}}/r_*) \rangle$. The problem here is determining the logarithm since we need to know the size of the BCG halo (as distinct from the cluster halo). This could be determined by galaxy-galaxy lensing, and also could in principle be determined from simulations.

A rough estimate can be obtained from tidal considerations: The BCG halo density is $\rho_{\text{halo}} \sim 3\sigma_*^2/4\pi G r_{\text{halo}}^2$ while the density of the cluster is $\rho_{\text{CL}} \sim 2\sigma_{\text{CL}}^2/4\pi G r^2$ where now r is the typical cluster-centric distance to the BCG. If this is a few hundred kpc then the tidal constraint that $\rho_{\text{halo}} \geq \rho_{\text{CL}}$ says that r_{halo} can't be bigger than about 1/3 of this. The scale lengths for BCGs are typically 10kpc, so this would suggest that the logarithm is approximately 2.5. If the halos are really this large, the effect of the motion of the stars $\delta z \simeq -3\sigma_*^2/2c^2$ is a small correction, and we have a net redshift $\delta z \simeq 1.25$ km/s/c.

5.3 Revised Prediction for Redshift Profile

We will proceed in two steps. We bootstrap off the estimate of the difference in potential between the BCG and the innermost point using the WHH stacked NFW model method. The innermost data point lies at $r_{\perp} = 0.6$ Mpc where the assumptions of virial equilibrium are likely to be well obeyed. We then extrapolate to larger impact parameters assuming galaxies trace the mass and using the cluster-galaxy cross-correlation function to get the appropriate ensemble average mass profile.

The stacked NFW model appears to provide a good fit to the data within 1.2 Mpc (WHH supplementary figure 2) and yields a potential for galaxies at impact parameter 0.6 Mpc corresponding to $\delta z_{\text{GR}} \simeq -5.0$ km/s/c. This was obtained after correcting the velocity dispersions for the motion of the BCGs, which we have argued above is inappropriate, so we should increase this accordingly by about 13%. The finite BCG velocities will reduce the gravitational potential difference by about 0.9 km/s/c but the BCG halo potential increases it by an estimated 1.6 km/s/c. The net result is a potential difference of $\delta z_{\text{GR}}(0.6 \text{ Mpc}) \simeq -6.4$ km/s/c.

We now need include the kinematic effects. The observed velocity dispersion at this impact parameter is $\sigma_{\text{obs}} \simeq 610$ km/s, so with $\sigma_{\text{BCG}} = 0.5\sigma_{\text{CL}}$ the LC and TD effects are $\delta z_{\text{TD+LC}} \simeq (3/5)2.5\sigma^2/c^2 = +1.9$ km/s/c. The SB effect for the non-BCGs is $\delta z_{\text{SB}} \simeq -10.0\sigma_{\text{CL}}^2/c^2 \simeq -9.9$ km/s/c and the SB effect on the BCGs we have estimated to be

about +1.9 km/s/c, and finally the kinematic blue-shift for the stars in the BCG gives +0.3 km/s/c for a net kinematic effect $\delta z_{\text{TD+LC+SB}}(0.6 \text{ Mpc}) \simeq -5.8$ km/s/c for a grand total $\delta z_{\text{GR+TD+LC+SB}}(0.6 \text{ Mpc}) \simeq -12.2$ km/s/c. whereas the observed value is $\delta z \simeq -2.6$ km/s/c. The uncertainty on this point is approximately 6 km/s/c so this would appear to be discrepant, but only at about the 1.5-sigma level.

The NFW model predicts $\delta z \simeq -10$ km/s/c for the outer measurements $r \simeq 3.3, 5.3$ Mpc, and the measurements straddle this value. While this model may provide a reasonable description for isolated clusters in the virialised domain, it is not at all clear that it is appropriate to describe the composite cluster being studied here. Tavio *et al.* (2008) have claimed that beyond the virial radius the density in numerical LCDM simulations actually falls off like $\rho \sim 1/r$ rather than the $\rho \sim 1/r^3$ asymptote for the NFW profile, and the extended peculiar in-fall velocities found by Ceccarelli *et al.* (2011) also argue for shallow cluster profiles, but it is not clear that these results are widely accepted.

An alternative, and possibly more reliable, approach is to assume that galaxies trace the mass reasonably well, in which case the density profile of the stacked cluster has the same shape as the cluster-galaxy cross correlation function (e.g. Croft *et al.*, 1997). This has a power-law dependence $\rho \sim r^{-\gamma}$ with $\gamma \simeq 2.2$, i.e. intermediate between the NFW and Tavio *et al.* model predictions.

For space density $\rho(r) = \rho_0(r/r_0)^{-\gamma}$, where r_0 is an arbitrary fiducial radius, the potential is $\Phi(r) = \Phi_0(r/r_0)^{2-\gamma}$ and the 1-D velocity dispersion, for isotropic orbits, is $\sigma^2(r) = \sigma_0^2(r/r_0)^{2-\gamma}$ with $\Phi_0 = 2((1-\gamma)/(2-\gamma))\sigma_0^2$.

The projected velocity dispersion measured is related to the 3-D velocity dispersion by $\sigma^2(r_{\perp})/\sigma^2(r) = \int dy y^{2-\gamma}(1+y^2)^{-\gamma/2}$ but the projected potential is related to the 3-D potential in the same way, so the projected quantities are related by $\Phi(r_{\perp}) = -2[1-\gamma]\sigma^2(r_{\perp})$. This is the potential relative to infinity. The difference in projected potential between two projected radii r_1 and r_2 is $\Phi(r_2) - \Phi(r_1) \simeq 2.4\sigma^2(r_1)(1 - (r_1/r_2)^{0.2})$ for $\gamma = 2.2$. The resulting GR effect is shown as the dashed line in figure 3 and is actually quite similar to the shape of the profile for the WHH NFW composite model.

The FWHM of the bell-shaped velocity distributions in WHH figure 1 appear to decrease by about 15% between the inner-bin and the outer points. This is reasonably consistent with the expected $\sigma^2 \propto r^{-0.2}$ trend predicted if galaxies trace mass, but this is perhaps fortuitous since the outer points are well outside the virial radius. Regardless of whether the galaxies at large radius are equilibrated or not, we can use the change in the observed velocity dispersion with radius to obtain the differential TD+LC+SB effect which is shown, added to the GR effect, as the solid line in figure 3. The kinematic effects flatten out the predicted profile, so the prediction is quite different from the gravitational redshift alone.

The situation is clearly rather complicated, especially when using BCGs as the origin of coordinates since the effects depend on things like the relative velocities of the top ranked pair of cluster galaxies, and on the BCG halo properties, that are quite poorly known. However, those factors only influence the prediction for the innermost data point. The empirically based theoretical prediction for the profile of the redshift offset for the hot population as a function

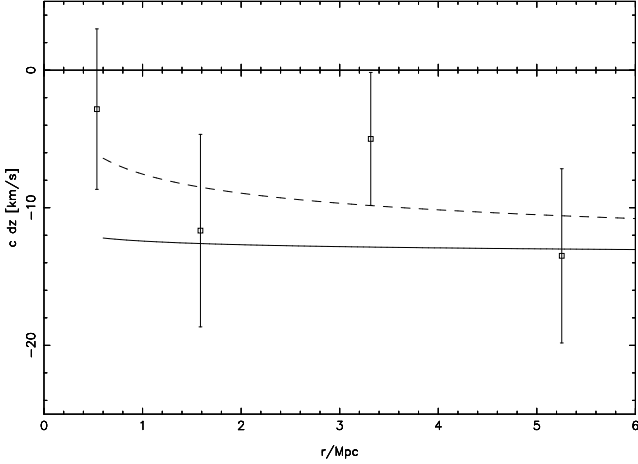


Figure 3. Data points from figure 2 of WHH and prediction based on mass-traces-light cluster halo profile and measured velocity dispersions as described in the main text. The dashed line is the gravitational redshift prediction, which is similar to the WHH model prediction. The solid curve includes, in addition, the kinematically sourced effects that are the main focus of this paper.

of impact parameter at $r_{\perp} > 0.6\text{Mpc}$ is the most robust; if galaxies are reasonable tracers of the mass then profile should be very flat, quite unlike the GR effect from a NFW profile. The predicted GR and total effects are shown in figure 3. However, this analysis ignores the effect of secular infall and out-flow which we consider next.

6 EFFECT OF INFALL AND OUTFLOW

The discussion so far has focused mostly on the stable, virialised regions. Clusters, however, are evolving structures and the mass within any fixed physical radius $M(r)$ will in general be changing. Outside of the virial radius (generally considered, inspired by the spherical collapse model, to be the radius within which the mean enclosed mass density is $3\pi/Gt^2$) we expect to see net infall, and the enclosed mass at those radii will be increasing with time, while at still larger radii there will be outflow tending asymptotically toward the Hubble flow. In the spherical collapse model the transition from inflow to outflow takes place at the turnaround radius where the mean enclosed mass density is $\bar{\rho}_t = 3\pi/32Gt^2$. This is for a matter dominated Universe; allowing for a cosmological constant makes only a small change (Lokas & Hoffman, 2001).

For the empirically motivated $\rho = \rho_0(r/r_0)^{-\gamma}$ model the mean enclosed mass is $\bar{\rho}(r) = 3(\gamma - 1)(2\pi G)^{-1}\sigma_0^2 r_0^{\gamma-2} r^{-\gamma}$ and the nominal virial radius is $r_{\text{vir}} = ((\gamma - 1)\sigma_0^2 r_0^{\gamma-2} t^2 / 2\pi^2)^{1/\gamma} \simeq 1.8\text{Mpc}$ using $\gamma = 2.2$, $r_0 = 1\text{Mpc}$, $\sigma_0 = 545\text{km/s}$ and $t \simeq 1/H = 1/(70\text{km/s/Mpc})$ and turnaround is at $r_t \simeq 8.7\text{Mpc}$.

In the centres of clusters there may be softening of the cores which would reduce the enclosed mass and would have an associated outflow.

In any single cluster, the density may be changing rapidly — on the local dynamical timescale — especially during mergers and as clumps rain in, but for a composite cluster such as considered here these rapid changes will

average out and the mass can only change on a cosmological timescale: $\dot{M} \sim HM$. For power law profile with $\gamma \simeq 2$ $M \simeq 4\pi\rho r^3$ and $\dot{M} \simeq 4\pi\rho^2\bar{v}$, where \bar{v} is the mean infall velocity, by continuity. So if $\dot{M}(r) = \alpha(r)HM(r)$, with, by the above argument, $\alpha(r)$ of order unity, then $\nabla(\mathbf{r}) = \alpha(r)H\mathbf{r}$.

This secular flow can generate a net offset for the redshifts in two ways. First, and most importantly for clusters at $Z \ll 1$, along any line of sight we observe galaxies that lie in a cone that will be wider at the back of the cluster. At low redshift this means there will be more galaxies observed at the back than the front in an intrinsically symmetric cluster. But we also need to allow for the countervailing bias caused by the fact that the more distant galaxies will be fainter which, as we have seen above, overwhelms the effect of the change of volume in the relevant range of redshifts. These geometric and flux limit effects, whose effects on the foreground and background galaxies was discussed by Kim and Croft (2004), modulate the density per unit line of sight distance linearly with distance. The real flux limited galaxies observed along cones behave like particles with no flux selection observed in cylinders with a phase space density $\rho'(\mathbf{r}, \beta) = \rho(\mathbf{r}, \beta)(1 + 2Hx(\delta(Z) - 1)/cZ)$.

We can try to use this to estimate the redshift offset as $\int dx \int d^3\beta \rho'(\mathbf{r}, \beta) \beta_x / \int dx \int d^3\beta \rho(\mathbf{r}, \beta)$. Performing the integrals over velocity this is

$$\langle \beta_x \rangle_{r_{\perp}} = \int dx \left(1 + \frac{2Hx}{cZ} (\delta(Z) - 1) \right) \rho(\mathbf{r}) \bar{\beta}_x(\mathbf{r}) / \int dx \rho(\mathbf{r}) \quad (24)$$

or, with $\bar{\beta}_x(\mathbf{r}) = \alpha(r)Hx/c$ and an assumed $\sim 1/r^2$ density profile,

$$\langle \beta_x \rangle_{r_{\perp}} = \frac{2H^2}{c^2 Z} (\delta(Z) - 1) \int dx \frac{\alpha(r)x^2}{r^2} / \int \frac{dx}{r^2} \quad (25)$$

where $r = \sqrt{r_{\perp}^2 + x^2}$. This is rather messy and, owing to the presence of the factor $\alpha(r)$, model dependent. But we can note the following: if we work at $r_{\perp} \sim 1\text{Mpc}/h$ say, the integral in the denominator will be $\sim 1/r_{\perp}$ while the contribution to the integral in the numerator from $-r_{\perp} < x < r_{\perp}$ will be $\sim r_{\perp} \alpha(r_{\perp})$, so we get a partial contribution to $\langle \beta_x \rangle_{r_{\perp}} \sim H^2 r_{\perp}^2 / c^2 Z \simeq 5 \times 10^{-7} Z_{0.2}^{-1}$, which is very small; corresponding to a physical velocity of only 0.16 km/s. If we extend the range of integration beyond $|x| < r_{\perp}$ this will increase, but not by a very large factor, since $\alpha(r)$ will start its decrease towards zero at the turnaround radius. Extending the range of integration still further the average decreases since α now has changed sign. Ultimately, the value of this integral will become large, and even more so beyond the $\sim 10\text{Mpc}/h$ scale of the cluster-galaxy cross-correlation function, but this would not be seen as a shift of the bell-shaped enhancement of the redshift distribution.

The secular infall or outflow can also couple to the time rate of change of the phase-space distribution function, which will also be changing on a cosmological timescale (both the density and the width of the velocity distribution will, in general, be varying). This will result in a formally similar contribution to the redshift offset, but without the factor $1/Z$, so for low-redshift clusters this will be still smaller.

At larger impact parameter the effect of outflow is more interesting. In figure 3 we show the line-of-sight velocity distribution for a simple, but plausible, model for cluster density and velocity structure in the out-flow region. The key

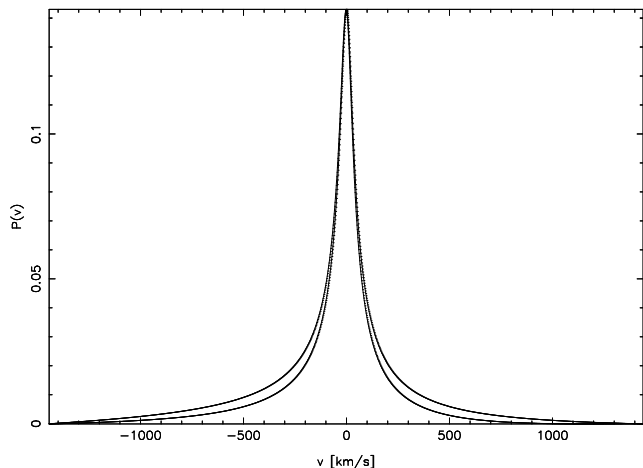


Figure 4. Distribution of line of sight velocities at impact parameter $r_{\perp} = 10\text{Mpc}$ for a simple model where $\xi_{\text{cg}} = (r/r_0)^{-2}$ with correlation length $r_0 = 10\text{Mpc}$ and turnaround radius $r_t = 8.7\text{Mpc}$ and where the velocity is $v = H(r - r_t)$. A linear ramp determined from the outermost points has been subtracted. These were generated using equation 13 with parameter $2H(\delta(Z) - 1)/cZ = 0$ (thin line) and $0.023/\text{Mpc}$ (thick line). This is highly exaggerated. For clusters at $Z = 0.2$, or averaged over the distribution of galaxy redshifts, this parameter is $\simeq 0.0023$. Scaling the mean velocity appropriately gives $\delta z \simeq -3.0\text{km/s/c}$. This is for cold spherical outflow. In reality this will be convolved with a broad quasi-Gaussian distribution of random velocities from local substructures but the shift of the centroid will be essentially the mean of the distribution shown here.

assumption here is that outside of turnaround the radial velocity is $v \simeq H(r - r_t)$ and is supported but the analysis of peculiar velocity profiles numerical simulations (Ceccarelli, *et al.*, 2011). The amplitude of the effect has been exaggerated in figure 4 by a factor 10 for clarity. For the average of $2H(\delta(Z) - 1)/cZ$ over the distribution of galaxy redshifts shown in figure 2 is approximately $0.0023/\text{Mpc}$. Scaling the the mean velocity from the model appropriately yields an expected blue-shift driven by the out-flow of about $\delta z \simeq -3.0\text{km/s/c}$ at impact parameter $r_{\perp} \simeq 10\text{Mpc}$. Over the range of impact parameters explored by WHH the effect of infall and outflow is very small.

7 DISCUSSION

We have shown that, in addition to the transverse Doppler effect, there are additional factors that need to be taken into account in interpreting the measurement of the offset of the net blue-shift of the cluster galaxies relative to the central brightest cluster galaxy. These are straightforward to estimate from the measured line-of-sight velocities and can therefore be subtracted from the measured blue-shift. The TD effect is a little more difficult to estimate, as it depends to some degree on the velocity dispersion anisotropy, but as it is a relatively small effect for the WHH experiment little error is made if we assume isotropic orbits. We have also shown that the redshift offset for unresolved sources is different again; the kinematically sourced effect is a blue-shift that is just the opposite of the standard transverse Doppler term.

We have applied these results to the WHH measurement. We have used an empirically motivated model for the composite cluster halo mass density profile together with the observed velocity dispersions to predict the net redshift offset. The largest correction comes from the surface brightness modulation effect. This is roughly equal to the GR effect at small impact parameters, and, since the velocity dispersion is falling with radius, this flattens out the blue-shift profile. The result, it has to be admitted, does not seem to agree as well with the data as the GR prediction alone.

The current data do not place particularly strong constraints on theories that invoke long-range non-gravitational interactions in the dark sector. However, the observational situation has already improved substantially with nearly three times as many galaxy redshifts obtained by the Sloan telescope once one includes the extensions such as BOSS (Dawson *et al.*, 2013), and in the near future there will be yet more data available, from surveys such as big-BOSS and also potentially from ASKAP and Aperitif in the radio (Duffy, *et al.*, 2012), to strengthen this test of fundamental physics.

ZPL suggested that, in principle, one could use the difference in redshift offsets observed for X-ray gas, assuming that can be done, and measurements of galaxies as a probe of the anisotropy of the velocity dispersion tensor in clusters. The analysis here shows that the strength of the kinematically sourced redshifts depends on the luminosity weighting scheme adopted, whereas, to the extent that the shape of the luminosity function is independent of position, this would not bias the measurement of the gravitational redshift. This provides, in principle, another way to constrain the orbital anisotropy.

8 ACKNOWLEDGEMENTS

The author enjoyed stimulating discussions on this subject with Bob McLaren, Harald Ebeling, William Burgett, Bill Unruh, Richard Ellis, and Alex Szalay, and is particularly grateful for useful input from Scott Tremaine and John Peacock. This study was aided by the support of Cifar.

REFERENCES

- Abazajian K. N., *et al.*, 2009, *ApJS*, 182, 543
- Bekenstein J. D., 2004, *PhRvD*, 70, 083509
- Bekenstein J. D., Sanders R. H., 2012, *MNRAS*, 421, L59
- Bernardi M., Hyde J. B., Sheth R. K., Miller C. J., Nichol R. C., 2007, *AJ*, 133, 1741
- Binney J., Tremaine S., 2008, *Galactic Dynamics Vol 2*
- Broadhurst T., Scannapieco E., 2000, *ApJ*, 533, L93
- Bunn E. F., Hogg D. W., 2009, *AmJPh*, 77, 688
- Ceccarelli L., Paz D. J., Padilla N., Lambas D. G., 2011, *MNRAS*, 412, 1778
- Coleman G. D., Wu C.-C., Weedman D. W., 1980, *ApJS*, 43, 393
- Coziol R., Andernach H., Caretta C. A., Alamo-Martínez K. A., Tago E., 2009, *AJ*, 137, 4795
- Croft R. A. C., Dalton G. B., Efstathiou G., Sutherland W. J., Maddox S. J., 1997, *MNRAS*, 291, 305
- Dawson K. S., *et al.*, 2013, *AJ*, 145, 10
- Duffy A. R., Meyer M. J., Staveley-Smith L., Bernyk M., Croton D. J., Koribalski B. S., Gerstmann D., Westerlund S., 2012, *MNRAS*, 426, 3385
- Farrar G. R., Rosen R. A., 2007, *PhRvL*, 98, 171302

- Gradwohl B.-A., Frieman J. A., 1992, ApJ, 398, 407
 Gubser S. S., Peebles P. J. E., 2004, PhRvD, 70, 123511
 Hansen S. M., Sheldon E. S., Wechsler R. H., Koester B. P., 2009, ApJ, 699, 1333
 Hao J., et al., 2010, ApJS, 191, 254
 Kasun S. F., Evrard A. E., 2005, ApJ, 629, 781
 Kim Y.-R., Croft R. A. C., 2004, ApJ, 607, 164
 Lokas, E. L., Hoffman, Y., 2001, in proceedings Identification of Dark Matter, eds. Spooner, N. J. C. and Kudryavtsev, V., arXiv:astro-ph/0011295
 Lynden-Bell D., 1967, MNRAS, 136, 101
 Maxwell, J. C., 1875, "Attraction", Encyclopedia Britannica Ninth Edition 3: 6365
 Misner, C.W., Thorne, K.S., Wheeler, J.A., 1973, Gravitation, W.H. Freeman, San Francisco, p1078
 Montero-Dorta A. D., Prada F., 2009, MNRAS, 399, 1106
 Navarro J. F., Frenk C. S., White S. D. M., 1997, ApJ, 490, 493
 Skibba R. A., van den Bosch F. C., Yang X., More S., Mo H., Fontanot F., 2011, MNRAS, 410, 417
 Smith G. P., et al., 2010, MNRAS, 409, 169
 Tavio H., Cuesta A. J., Prada F., Klypin A. A., Sanchez-Conde M. A., 2008, arXiv:0807.3027
 Will, C.M., 2006, Living Reviews of Relativity, 9, 3
 Wojtak R., Hansen S. H., Hjorth J., 2011, Nature, 477, 567
 Zhao, H., Peacock, J.A., Li, B., 2012. arXiv:1206.5032

APPENDIX A: PREDICTING THE REDSHIFT DISTRIBUTION

We have estimated above the effects on the mean redshift. However, what is actually measured is not a simple centroid, since there are foreground and background galaxies so what WHH did was to fit the distribution of redshifts relative to the BDG to a model with a background consisting of a linear ramp and a cluster consisting of a double Gaussian. Given a theoretical model for the PSD, either analytic or obtained by stacking clusters found in a simulation, one would like to generate the predicted distribution of redshifts as a function of impact parameter. A convenient way to do this is to note that the observed redshift z expressed as a recession velocity is, as before, $\beta'_x = -z = \beta_x - \beta_x^2/2 - \beta_\perp^2/2 + \Phi/c^2$, where we have now separated β^2 into line of sight and transverse components. Thus $d\beta'_x = (1 - \beta_x)d\beta_x$; i.e. the Jacobian of the transformation from velocity β , with respect to the rest-frame observers, to measured redshift β' is $1 - \beta_x$. Conservation of particles requires that the observed density of particles as a function of position, redshift and transverse velocity $\rho'(\mathbf{r}, \beta'_x, \beta_\perp)$ satisfies $\rho'(\mathbf{r}, \beta'_x, \beta_\perp)d\beta'_x = \rho_{LC}(\mathbf{r}, \beta_x, \beta_\perp)d\beta_x$ so

$$\rho'(\mathbf{r}, \beta'_x, \beta_\perp) = \rho_{RF}(\mathbf{r}, \beta'_x + \beta_x^2/2 + \beta_\perp^2/2 - \Phi/c^2, \beta_\perp) \quad (\text{A1})$$

i.e. the density of objects in position, radial and transverse velocities is a mapping of the rest-frame PSD with a displacement along the β_x axis. Note that β_\perp^2 here denotes the sum of the squares of the two transverse velocity components.

We can now expand the RHS as a Taylor series for small displacement. We also want to evaluate this at $t = x/c$, which we can also treat as a small displacement, resulting

in

$$\begin{aligned} \rho'(\mathbf{r}, \beta_x, \beta_\perp) &= \rho(\mathbf{r}, \beta_x, \beta_\perp) \\ &+ (\beta_x^2/2 + \beta_\perp^2/2 - \Phi/c^2) \frac{\partial \rho(\mathbf{r}, \beta_x, \beta_\perp)}{\partial \beta_x} \\ &+ \frac{x}{c} \dot{\rho}(\mathbf{r}, \beta_x, \beta_\perp) \end{aligned} \quad (\text{A2})$$

where dot denotes partial derivative with respect to time, and we have dropped the prime on β_x . Integrating over the transverse velocity components gives

$$\begin{aligned} \rho'(\mathbf{r}, \beta_x) &= \rho(\mathbf{r}, \beta_x) \\ &+ (\beta_x^2/2 + \langle \beta_\perp^2 \rangle/2 - \Phi/c^2) \frac{\partial \rho(\mathbf{r}, \beta_x)}{\partial \beta_x} \\ &+ \frac{x}{c} \dot{\rho}(\mathbf{r}, \beta_x). \end{aligned} \quad (\text{A3})$$

As a sanity check, if we ignore the last term, multiply by β_x , and integrate over space and velocity, assuming ρ to be an even function of its arguments, we find $\delta z = \langle -\beta_x \rangle = \langle \beta_x^2 \rangle + \langle \beta_x^2 + \beta_\perp^2 \rangle/2 - \Phi/c^2$ in accord with equation (5).

We could integrate this expression over line of sight distance to get the distribution function for the observed redshift as a function of the impact parameter, but that would not properly allow for the fact that we observe in a cone, nor would it incorporate the surface brightness boosting effects. Both of these can be allowed for simply by multiplying the first term on the RHS by the factors $1 + (3 + \alpha(Z))\delta(Z)\beta_x$ and $1 - 2Hx(\delta(Z) - 1)/cZ$. Linearising the result gives:

$$\begin{aligned} \rho'(\mathbf{r}_\perp, \beta_x) &= \rho(\mathbf{r}_\perp, \beta_x) + \int dx \{ \\ &(\beta_x^2/2 + \langle \beta_\perp^2 \rangle/2 - \Phi/c^2) \frac{\partial \rho(\mathbf{r}, \beta_x)}{\partial \beta_x} \\ &+ ((3 + \alpha(Z))\delta(Z)\beta_x - 2Hx(\delta(Z) - 1)/cZ) \rho(\mathbf{r}, \beta_x) \\ &+ \frac{x}{c} \dot{\rho}(\mathbf{r}, \beta_x) \}. \end{aligned} \quad (\text{A4})$$

This is valid for an individual cluster. If we average over the population of clusters and denote averaged properties as e.g. $\bar{\rho} = \int dC P(C) \rho / \int dC P(C)$ then we have

$$\begin{aligned} \bar{\rho}'(\mathbf{r}_\perp, \beta_x) &= \bar{\rho}(\mathbf{r}_\perp, \beta_x) + \int dx \{ \\ &\frac{\beta_x^2}{2} \frac{\partial \bar{\rho}(\mathbf{r}, \beta_x)}{\partial \beta_x} + \frac{\partial}{\partial \beta_x} (\langle \beta_\perp^2 \rangle/2 - \Phi/c^2) \bar{\rho}(\mathbf{r}, \beta_x) \\ &+ ((3 + \alpha(Z))\delta(Z)\beta_x - 2Hx(\delta(Z) - 1)/cZ) \bar{\rho}(\mathbf{r}, \beta_x) \\ &+ \frac{x}{c} \dot{\bar{\rho}}(\mathbf{r}, \beta_x) \}. \end{aligned} \quad (\text{A5})$$

With an ensemble average cluster PSDF, along with the average of this times $\langle \beta_\perp^2 \rangle/2 - \Phi/c^2$ from e.g. a cosmological simulation this expression, after integrating along the line-of-sight, provides the predicted distribution function for the observed redshifts which can then be analysed in precisely the same way at the real data (e.g. finding the shift of the velocity distribution by modelling) to obtain the predicted redshift offset as a function of impact parameter. This would also allow comparison of predicted and observed higher order moments of the velocity distribution such as skewness and kurtosis.